Canadian Journal of Physics

Article

Half-metallicity from CrCoSi and MnCoSi half-Heusler alloys to their derivative double half-Heusler $CrMnCo_2Si_2$

Hiba Elarabi[a], Friha Khelfaoui[a], Keltouma Boudia[b], Fatima Labani[a], Mama Hamlat[a], Ouafaa Sadouki[b], Fadila Belkharroubi[c], Fares Faid[d], Abdelmadjid Bouhemadou[e], and Bahri Deghfel[f]

[a]Laboratory of Physicochemical Studies, University of Saida-Dr. Moulay Tahar, Saida 20000, Algeria; [b]University of Tissemsilt, Ahmed Ben Yahia El-Wanchrissi, Algeria; [c]Laboratory of Physical Chemistry of Advanced Materials (LPCMA), University of Djillali Liabes, BP 89, 22000, Sidi-Bel-Abbes, Algeria; [d]Common Trunk Sciences and Technology Department, Faculty of Technology, University of Laghouat, Algeria; [e]Laboratory for Developing New Materials and their Characterizations, University of Ferhat Abbas Setif 1, Faculty of Sciences, Department of Physics, Setif 19000, Algeria; [f]Department of Physics, Faculty of Sciences, University of M'sila, Algeria

Corresponding author: **Friha Khelfaoui** (email: friha.khelfaoui@univ-saida.dz)

Abstract

The structural, elastic, electronic, and magnetic properties of the CrCoSi, MnCoSi parent half-Heusler (HH) alloys, and their $CrMnCo_2Si_2$ derivative double half-Heusler (DHH) compound are studied, utilizing the augmented plane wave method, which is based on density functional theory and implemented in the WIEN2k code. The stability of HH structure of the CrCoSi and MnCoSi alloys has been checked for their non-magnetic and ferromagnetic phases, leading to that the latter phase of the type I arrangement is the most stable. The $CrMnCo_2Si_2$ DHH alloy, derivative from the found structural and magnetic ground states of CrCoSi and MnCoSi HH alloys, is constructed and investigated. This DDH as well as its CrCoSi parent HH are found to be resistant to deformation and can be classified as ductile materials, whereas the MnCoSi compound is brittle. By the gradient generalized approximation (GGA), the electronic structures of CrCoSi, MnCoSi, and $CrMnCo_2Si_2$compounds exhibit a metallic behavior in the spin-up channel and a semiconducting behavior in the spin-dn channel, with band gaps (half-metallic gaps) of 0.851(0.020), 0.852(0.021), and 0.531(0.002) eV, respectively. The half-metallicity of $CrMnCo_2Si_2$ DHH is retained with smaller (larger) band gap (half-metallic gap) of 0.38(0.106) eV than that of GGA, using GGA + U approximation. In addition, the total magnetic moments are found to be 1, 2, and 3 μ_B for CrCoSi, MnCoSi, and $CrMnCo_2Si_2$, respectively. Therefore, these alloys can be good candidates for spinitronic applications due to their half-metallicity.

Key words: half-metal, heusler alloys, spin polarization, mechanical stability, FP-LAPW

1. Introduction

Spin-based electronics has grown into a significant field of study that spans a wide range of high spin-polarized materials, used in spintronic devices. It overcomes the limitations of electronics by using the spin-to-store information instead of charge of electrons. The half-metallic ferromagnets (HMFs) are an important class of spintronic materials with a very unique electronic structure. In these materials, electrons with one spin orientation pass through the Fermi surface to participate in conduction, showing a metallic character; while the electrons with the other spin orientation exhibit insulator or semiconductor characteristics [1, 2].

Therefore, the half-metals have theoretically a spin polarization of 100% and can provide fully spin-polarized carriers. They are regarded as ideal materials for the construction of spintronic devices and have attracted much attention. Heusler alloys [3] are one of the most motivating category of materials with half-metallic behavior, which structurally have many possible types: full-Heusler alloys with general formula X_2YZ, half-Heusler (HH) with formula XYZ, and quaternary compound with the composition XX′YZ. Several Heusler alloys have been investigated and found to be HMFs, such as that of de Groot et al. 1983 [4], where they have shown that the most famous HH, NiMnSb compound, is a half-metallic ferromagnetic (FM) material, using the magnetic measurements [5]. The first prediction of this phenomenon, in the case of quaternary and full Heusler compounds, has been found by the Japanese research groups; Ishida et al. studied the Co_2MnZ compounds, where Z matches to Si and Ge [6] and Alijani et al. have demonstrated that the quaternary intermetallic Heusler compounds CoFeMnZ (Z = Al, Ga, Si, or Ge) are potential HMFs with high Curie temperatures, using ab initio electronic structure calculations [7]. Another renowned class of HMFs is found in the rutile structure like the magnetic oxide Fe_3O_4 [8] and CrO_2 [9]. Galanakis et al. showed that zinc-blende compounds have a FM half-metallic behavior for a wide range of lattice constants [10]. The same behavior appears in double perovskite Sr_2CrReO_6 [11].

One of the Heusler family's well-known HMFs or near-HMFs is the HH alloys. Recently, the investigation of Uto et al. [12],

Fig. 1. Total energy per formula unit of ferromagnetic (FM), non-magnetic (NM), and antiferromagnetic (AFM) phases as functions of the volume for CrCoSi and MnCoSi HH alloys.

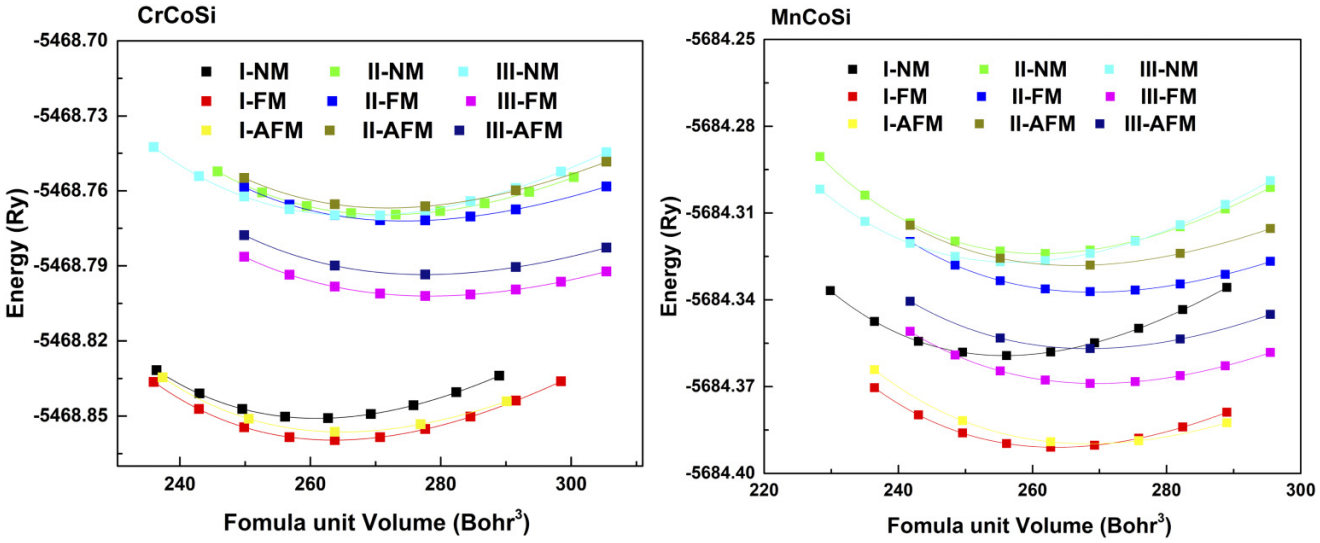

using density functional theory (DFT) calculations, indicate that CoCrSb is mechanically stable and has a half-metallic behavior, with a minority-spin band gap of 0.81 eV. Furthermore, Javed et al. [13] have calculated the spin-polarized band structures, cohesive formation energy, elastic constants, and have also analyzed the phonon dispersion curve of CrMnS HH to prove its half-metallic FM behavior, thermodynamically, mechanically, and dynamical stabilities. Latest DFT simulations by Ozdemir et al. [14] indicated a half-metallic behavior in MnZrX HH compounds (X = In, Tl, C, Si, Ge, Sn, Pb, N, P, As, Sb, O, S, Se, Te) [21].

In all above mentioned materials, the half-metallic character is caused by the d-spin polarization of the transition elements. Inspired by HH alloys, particularly those based on transition metals, and with the aim of enhancing literature with novel (HMFs) materials that have high spin polarization, we have studied novel double half-Heusler (DHH) $CrMnCo_2Si_2$, derivative from the HH alloys CrCoSi and MnCoSi, which have also been examined and compared with the results of Hussain [15], and Feng et al. [16]. In this paper, the outcomes of these latter are also compared with those of the considered novel DHH compound $CrMnCo_2Si_2$.

2. Computational method

In this paper, the full potential linearized augmented plane wave (FP-LAPW) method [17], within the framework of the DFT, as implemented in WIEN2k code [18], was used to examine the structural, mechanical, and magneto-electronic properties of CrCoSi, MnCoSi, and $CrMnCo_2Si_2$ Heusler alloys. The generalized gradient approximation (GGA) of Perdew–Burke–Ernzerhof [19, 20] was used to evaluate the exchange-correlation energy functional, for all considered materials, but for only $CrMnCo_2Si_2$ DHH compound, the Hubbard correction is added to the GGA (i.e., GGA + U), with the effective values (U_{eff}) of 1.59, 1.92, and 1.69 eV for Cr, Co, and Mn atoms, respectively. It has been demonstrated that these U_{eff} values are accurate for describing the magnetic moment and electronic structure in the Heusler alloys [21]. In this method, the space is divided into non-overlapping muffin-tin (MT) spheres separated by an interstitial region, and the used MT radii for Cr, Mn, Co, and Si atoms are 1.46, 1.71, 1.83, 1.5, and 1.71 (Bohr), respectively. In addition, the set cut-off parameters $R_{MT}.K_{max}$, l_{max}, G_{max}, and $N_{k\text{-points}}$ are 8.0, 10, 12, and 3000, respectively, where R_{MT} represent the smallest MT sphere radius, K_{max} is the maximum modulus for the reciprocal vectors, l_{max} is the maximum angular quantum number for the expansion of wave functions inside the spheres, G_{max} is the plane-wave cutoff (magnitude of largest vector in charge density Fourier expansion), and $N_{k\text{-points}}$ is the number of k-points in the whole Brillouin zone. The convergence criterion of 10^{-6} Ry and 10^{-5} e for the energy and charge, respectively, is used.

3. Results and discussion

3.1. Structural properties

The most important step in ab initio calculations is the determining of the structural properties for a given system on its ground state, which will enable us to understand other important physical properties. $CrMnCo_2Si_2$ crystallizes in a tetragonal structure with a space group N°115, generated from the two HH compounds CrCoSi and MnCoSi. The energy versus volume, for latter compounds (i.e., HH) in their FM, non-magnetic (NM), and antiferromagnetic (AFM) phases, is calculated in the first step and shown in Fig. 1. These graphs show that our HH compounds are more stable in FM phase of type I (i.e., specified atomic arrangement: Cr/Mn(0,0,0), Co(1/4,1/4,1/4), Si(1/2, 1/2,1/2)) structure than the other phases because the corresponding energy is the

Fig. 2. Total energy per formula unit as functions of the volume for the ferromagnetic (FM), non-magnetic (NM), and antiferromagnetic (AFM) phases of $CrMnCo_2Si_2$ DHH alloy.

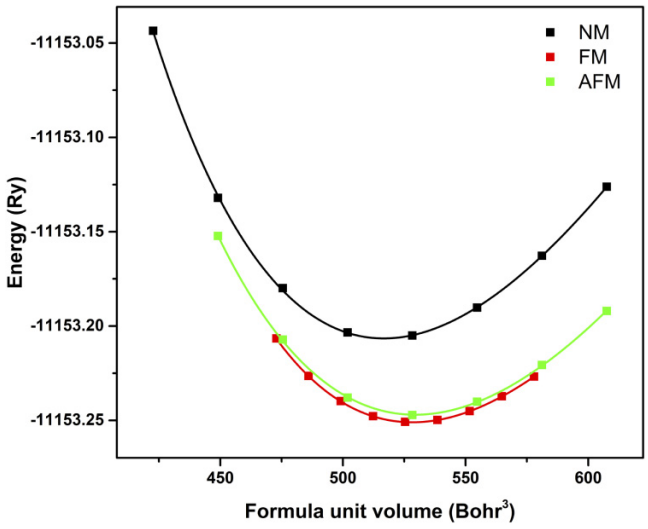

lowest. From this type structure, the DHH structure is obtained by substitution of two Cr atoms, in the cubic conventional cell of CrCoSi HH (lattice parameter a_{HH}), with Mn atoms. Therefore, the obtained structure has a tetragonal structure ($a_{DHH} = \frac{a_{HH}}{\sqrt{2}}$, $c_{DHH} = a_{HH}$). The optimization of this obtained DHH structure is performed for its FM, NM, and AFM phases, as shown in Fig. 2. As can be seen from this figure, the FM phase is the most stable magnetic phase. In addition, to obtain the ground state properties, the calculated total energies as functions of volume are fitted with the Birch–Murnaghan equation [22], as follows:

$$E(V) = E_0 + \frac{9V_0B_0}{16}\left\{\left[\left(\frac{V_0}{V}\right)^{2/3} - 1\right]^3 \grave{B}_0 + \left[\left(\frac{V_0}{V}\right)^{2/3} - 1\right]^2\left[6 - 4\left(\frac{V_0}{V}\right)^{2/3}\right]\right\} \quad (1)$$

Our calculated equilibrium lattice constants, bulk moduli B, pressure derivatives B′, and formation energies E_{form} are presented in Table 1. The bulk modulus is a measure of how resistant these compounds are to compression and is determined by the equation, $B = V\frac{\partial^2 E}{\partial V^2}$. The obtained results, as can be seen in Table 1, show that the resistance to compression (Bulk modulus) decreases with the increase of X atomic number (B(CrCoSi)> B($CrMnCo_2Si_2$)> B(MnCoSi)).

To verify the validity of synthesizing these alloys, we calculated the energy of formation using the following expressions:

$$E_{form}(XCoSi) = E^{tot}_{XCoSi} - \left(E^{bulk}_{X} - E^{bulk}_{Ca} - E_{Si}\right) \quad (2)$$

$$E_{form}(CrMnCo_2Si_2) = E^{tot}_{CrMnCo_2Si_2} - \left(E^{bulk}_{Cr} + E^{bulk}_{Mn} + 2E^{bulk}_{Ca} + 2E_{Si}\right) \quad (3)$$

where E^{tot}_{XCoSi} and $E^{tot}_{CrMnCo_2Si_2}$ are the total energies per unit cell for XCoSi(X = Cr and Mn) and $CrMnCo_2Si_2$, respectively, at the equilibrium state and E^{bulk}_{Cr}, E^{bulk}_{Mn}, E^{bulk}_{Co}, andE^{bulk}_{Si} match to the total energy for Cr, Mn, Co, and Si per atom, respectively, at ground state. The resulted negative values of the formation energy point out that our studied compounds are thermodynamically stable and it is possible to synthesize them experimentally.

To check the dynamical stability of the $CrMnCo_2Si_2$ compound, we calculated its phonon dispersion diagram using the linear response method within the density functional perturbation theory, as implemented in the CASTEP code [23]. The calculated phonon dispersion along lines of high symmetry in the Brillouin zone, for $CrMnCo_2Si_2$, is presented in Fig. 3. It is known that the absence of soft modes (imaginary modes, negative frequencies) in the phonon dispersion curve of a material implies its dynamical stability [24]. There are no negative frequencies in the phonon dispersion diagram, shown in Fig. 3, which highlights the dynamical stability of the $CrMnCo_2Si_2$ compound.

3.2. Mechanical properties

With a view to affirm the stabilization of our studied compounds, the elastic properties are performed using IRelast package, incorporated in WIEN2k code. The gained results reported in Table 2 are positive and obey Born's stability criteria for cubic structures [25]: $C_{11} > 0$, $C_{11} - C_{12} > 0$, $C_{11} + 2C_{12} > 0$, and $C_{44} > 0$, and for tetragonal (I) structures [26]: $C_{11} > 0$, $C_{33} > 0$, $C_{44} > 0$, $C_{66} > 0$, $C_{11} - C_{12} > 0$, $C_{11} + C_{33} - 2C_{13} > 0$, $2C_{11} + C_{33} + 2C_{12} + 4C_{13} > 0$, subsequently, CrCoSi, MnCoSi, and $CrMnCo_2Si_2$ are mechanically stable.

Other mechanical quantities, such as bulk $B_{C/T}$ (C for cubic structure and T for tetragonal structure), shear G, Young's moduli E, anisotropic factor, as well as Poisson's ratio, can be obtained from the evaluated elastic constants by using the following formula:

$$B_C = \frac{C_{11} + 2C_{12}}{3}, \quad B_T = \frac{1}{9}(2C_{11} + 2C_{12} + 4C_{13} + C_{33}) \quad (4)$$

$$G_C = \frac{1}{5}(3C_{44} + C_{11} - C_{12}) \quad (5)$$

$$G_T = \frac{1}{2}\left[\frac{2C_{11} + C_{33} - C_{12} - 2C_{13}}{15 + (2C_{44} + C_{66})/5} + \frac{15}{4(S_{11} + S_{22} + S_{33}) + 3(S_{44} + S_{55} + S_{66}) - 4(S_{12} + S_{13+}S_{23})}\right] \quad (6)$$

$$E_{C/T} = \frac{9BG}{3B + G} \quad (7)$$

$$\nu_{C/T} = \frac{1}{2}\left(1 - \frac{E}{3B}\right) \quad (8)$$

$$A_C = \frac{2C_{44}}{C_{11} - C_{12}}A_{C/T} = 5\frac{G_V}{G_R} + \frac{B_V}{B_R} - 6 \quad (9)$$

where B_V, G_V, B_R, and G_R are the estimated bulk and shear modulii by Voigt and Reuss methods, respectively. The calculated elastic constants as well as mechanical parameters, for all considered materials, are illustrated in Table 2 It can be seen that the bulk modulus values resulting through the elastic constants for the three compounds accord well with that gained from the total energy optimization. According

Table 1. Calculated lattice parameters (in Å) for the structural ground state of the CrCoSi, MnCoSi HH alloys and parent structure of $CrMnCo_2Si_2$ DHH, bulk modulii (in GPa), their derivative pressures, and formation (E_{form}) energies (in eV/atom) of the structural and magnetic ground phase (FM) for CrCoSi, MnCoSi, and $CrMnCo_2Si_2$ compounds.

X		a_{HH}	B	B'	E_{tot}	E_{form}
CrCoSi	GGA	5.3864 5.4100 [15] 5.3900 [16]	190.87	4.86	−5468.85962	−0.45
MnCoSi	GGA	5.3857 5.4100 [16]	174.72	5.02	−5684.39097	−0.44
$CrMnCo_2Si_2$	GGA	5.3899	181.00	4.72	−11153.250925	−0.45

Fig. 3. Phonon dispersion diagram along lines of high symmetry in the Brillouin zone for the $CrMnCo_2Si_2$ compound.

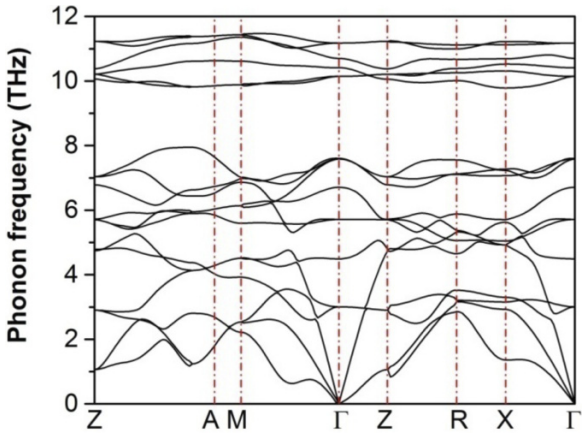

to the calculated datum, CrCoSi has a stronger capability to resist deformation compared with other compounds. Otherwise, the shear modulus presents a strong ability to defend versus reversible deformation by shear strain for $CrMnCo_2Si_2$ DHH alloy, while its young modulus value shows a greater hardness than their parent HH CrCoSi and MnCoSi.

To categorize ductility and brittleness of our studied compound, the B/G ratio, called Pugh's ratio, too is usually used. Depending on Pugh's [27] index, if $B/G < 1.75$ ($B/G > 1.75$), the material is characterized by brittle nature, otherwise, the ductile nature is expected. The calculated value of B/G was found to be 1.9, 1.7, and 1.9 for CrCoSi, MnCoSi, and $CrMnCo_2Si_2$, respectively. One can look out that MnCoSi is categorized as brittle, while CrCoSi and $CrMnCo_2Si_2$ compounds are showing their ductility.

The analysis of the degree of anisotropy requires the use of anisotropic parameter A. For isotropic materials $A = 1$; however for anisotropic materials $A \neq 1$ [28]. With regard to compounds CrCoSi, MnCoSi, and $CrMnCo_2Si_2$, it is found to be different to unity, so, these Heusler alloys have an anisotropic behavior. Poisson's ratio ν is ordinarily utilized to comprehend the kind of the bonding force in a compound [29]. The value of Poisson's ratio was evaluated to be 0.28, 0.26, and 0.27 for CrCoSi, MnCoSi, and $CrMnCo_2Si_2$, respectively, is around 0.25, indicating a higher ionic behavior as interatomic bonding. The resulted computed elastic parameters are, as shown in Table 2, in good agreement with those of Feng et al. [16] and Hussain et al. [15], for both investigated HH alloys.

3.3. Electronic and magnetic properties:

This section was used to comprehend the behavior of the electronic states of the CrCoSi and MnCoSi HH alloys and their derivative DHH $CrMnCo_2Si_2$ from their calculated band structures and density of state (DOS) maps, using GGA approximation, which are plotted for both spin channels. As shown in Fig. 4, it is clear that the general band profiles are almost analogous for both studied HH with a little diversity in the details. It can be seen band crossings with the Fermi level in the majority-spin channel, whereas in the minority-spin bands, the Fermi level just situated in the energy band gap, describing the considered HHs as half-metals with energy gaps (half-metallic gaps) of about 0.85(0.02) eV for both of them. This similarity is due to their very close atomic numbers of Cr (Z = 24) and Mn (Z = 25) atoms. In addition, as can be seen from Table 3, these findings are smaller than those of Feng el al [16] and Hussain et al. [15] due to different used methods, based on the description of the interaction between ions and electrons by ultrasoft pseudo potentials [30, 31]. Furthermore, our investigated derivative DHH $CrMnCo_2Si_2$ has much smaller gaps (HM gap) of 0.53(0.002) and 0.382(0.106) eV, obtained by GGA and GGA + U approximations, respectively. Thus, the obtained data demonstrate the half-metallic character of CrCoSi, MnCoSi, and $CrMnCo_2Si_2$ Heusler alloys, as indicated in Table 3.

To comprehend the electronic properties, total (TDOS) and partial (PDOS) densities of states have been plotted and given in Fig. 5. The magnetic moment is essentially originated from Cr and Mn atoms in which the Cr-d and Mn-d states have large exchange divisions between the states of the spin-up and -down channels around the Fermi level for CrCoSi and MnCoSi, respectively, as shown in Table 4. In addition, Co atom has a negative magnetic moment for both HH alloys, demonstrating an antiferomagnetic interaction between Co and Cr/Mn atoms. There is no contribution of Si atom for all studied Heusler compounds. The total magnetic moments are found to be 1 and 2 μ_B for CrCoSi and MnCoSi, respectively, but, for their derivative $CrMnCo_2Si_2$ DHH alloy, the results of both approximations (i.e., GGA and GGA + U) show that the main contribution to its total magnetic moment is from

Table 2. Elastic constants C_{11}, C_{12}, C_{13}, C_{33}, C_{44},C_{66} (in GPa), bulk B, Young E (GPa), shear G moduli (in GPa), B/G, anisotropic parameter A, and Poisson's coefficients υ of CrCoSi, MnCoSi, and $CrMnCo_2Si_2$ Heusler alloys.

X	C_{11}	C_{12}	C_{13}	C_{33}	C_{44}	C_{66}	B	E	G	B/G	A	υ
CrCoSi	285.5 274.6 [15]	145.8 115.2 [15]	–	–	132.3 94.9 [15]	–	192.4	125.8	49.3	1.9	0.62	0.28
MnCoSi	253.60	137.97	–	–	127.5	–	176.5	131.9	52.1	1.7	0.75	0.26
$CrMnCo_2Si_2$	330.96	74.15	137.7	268.2	127.5	65.2	181.0	248.0	97.5	1.9	0.57	0.27

Fig. 4. Spin-polarized band structures for CrCoSi, MnCoSi, and $CrMnCo_2Si_2$ Heusler alloys.

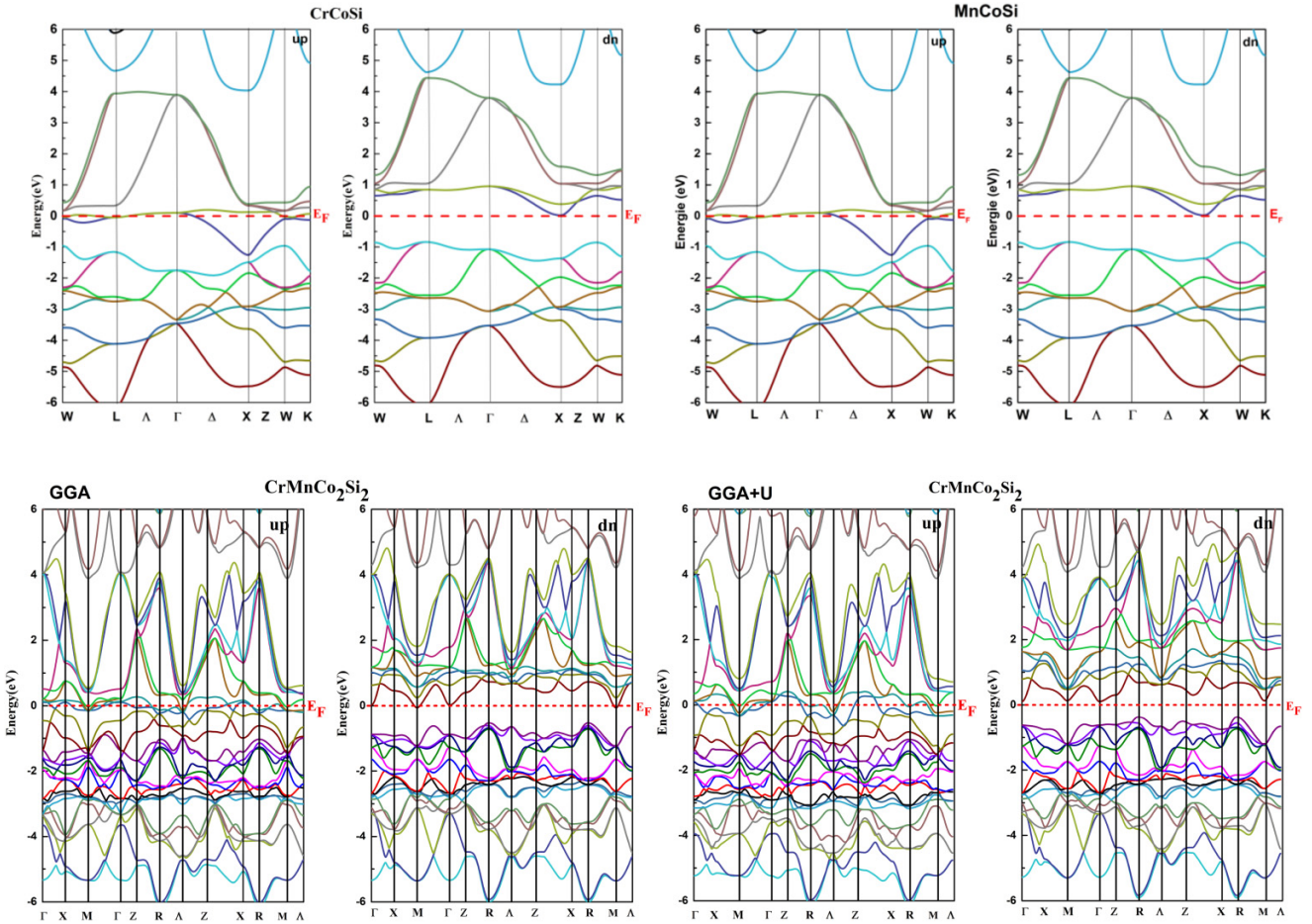

Table 3. Gap and half-metallic gap (in eV) of CrCoSi, MnCoSi, and $CrMnCo_2Si_2$ Heusler alloys.

X		Gap	HM gap
CrCoSi	GGA	0.851 1.160 [15] 0.670 [16]	0.020 0.650 [15] 0.660 [16]
MnCoSi	GGA	0.852 0.640 [16]	0.021 0.190 [16]
$CrMnCo_2Si_2$	GGA	0.53	0.002
	GGA + U	0.382	0.106

Cr and Mn atoms, as demonstrated by large splitting of their d-orbitals around Fermi level, leading to 100% spin polarization. Furthermore, little contributions to the total magnetic moment are from Co and Si atoms. The spin magnetization has an integer of 3 μ_B for $CrMnCo_2Si_2$, confirming its classification as half-metallic material.

4. Conclusion

Using FP-LAPW method, the structural, elastic, electronic, and magnetic properties of CrCoSi, MnCoSi, and $CrMnCo_2Si_2$ have been investigated. According to our calculations, they are stable in their FM phase. When compared with other compounds, CrCoSi's bulk modulus shows a higher resistance to the deformation. Otherwise, a large shear modulus value indicates a strong ability to defend against reversible deformation by shear strain for The DHH $CrMnCo_2Si_2$. The B/G values indicate the brittleness of MnCoSi, whereas CrCoSi, and $CrMnCo_2Si_2$ compounds are showing their ductility. The anisotropic coefficient A is different from the

Fig. 5. Spin-polarized density of states (DOS) for CrCoSi, MnCoSi, and $CrMnCo_2Si_2$ Heusler alloys.

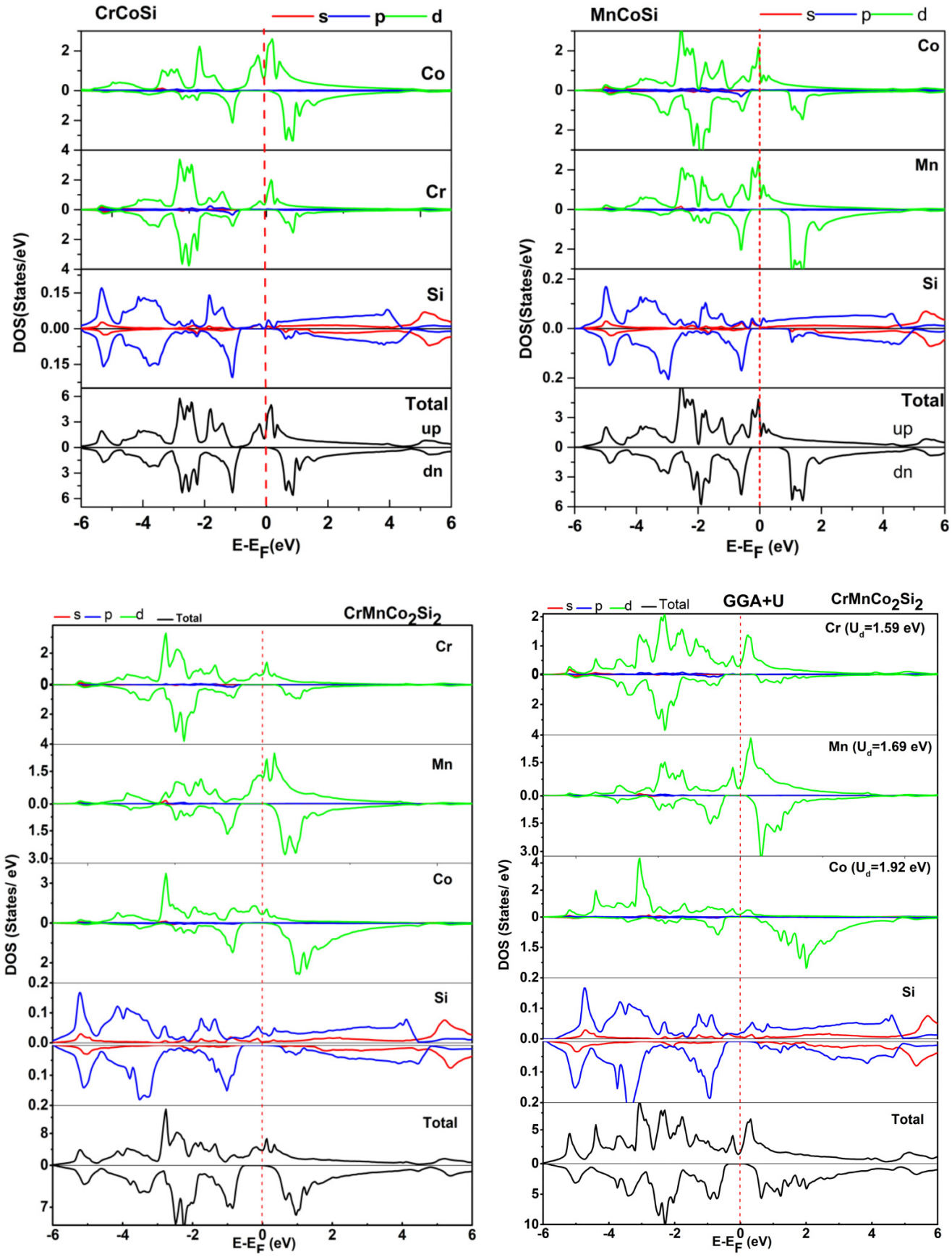

Table 4. Atomic (M_{Cr}, M_{Co}, M_{Mn}, M_{Si}), interstitial ($M_{Intersti}$), and total magnetic (M_{tot}) moments (in μ_B) for CrCoSi, MnCoSi, and $CrMnCo_2Si_2$ Heusler alloys.

X	Method	M_{Cr}	M_{Mn}	M_{Co}	M_{Si}	$M_{Intersti}$	M_{tot}
CrCoSi	GGA	1.166	–	−0.178	−0.031	0.043	1.000
		1.550 [15]		−0.410 [15]	−0.09 [15]		1.000 [15]
		1.560 [16]		−0.42 [16]			1.000 [16]
MnCoSi	GGA	–	2.114	0.027	−0.061	0.080	1.999
			2.120 [16]	−0.040 [16]			2.000 [16]
$CrMnCo_2Si_2$	GGA	0.612	2.560	−0.042	−0.034	−0.018	3.000
	GGA + U	0.438	3.352	−0.329	−0.058	−0.047	3.000

unit for all compounds, so, CrCoSi, MnCoSi, and $CrMnCo_2Si_2$ compounds have an anisotropic behavior. Poisson's ratio values of 0.28, 026, and 0.27 for CrCoSi, MnCoSi, and $CrMnCo_2Si_2$, indicate a higher ionic behavior as inter-atomic bonding. The electronic structures of CrCoSi, MnCoSi, and $CrMnCo_2Si_2$ exhibit a metallic behavior for the spin-up channel and a semiconducting behavior in the spin-dn channel. The integer values of 1 μ_B (CrCoSi), 2 μ_B (MnCoSi), and 3 μ_B ($CrMnCo_2Si_2$) confirm their half-metallic nature with a major contribution of Cr and Mn atoms. The 100% spin polarization of CrCoSi, MnCoSi, and $CrMnCo_2Si_2$ systems make all of them good candidates for spinitronic applications.

Article information

History dates

Received: 30 August 2022
Accepted: 2 January 2023
Version of record online: 18 May 2023

Copyright

Data availability

Data generated or analyzed during this study are provided in full within the published article.

Author information

Author contributions

Conceptualization: FK
Data curation: FK
Formal analysis: HE, FF, AB, BD
Investigation: HE, FB
Methodology: KB, OS
Project administration: KB, FL
Resources: KB
Software: FL
Supervision: FK, FL
Validation: OS
Visualization: HE
Writing – original draft: HE
Writing – review & editing: FK, KB, MH, FB, AB, BD

Competing interests

The authors declare there are no competing interests.

References

1. A. Aguayo and G. Murrieta. J. Magn. Magn. Mater. **323**, 3013 (2011). doi:10.1016/j.jmmm.2011.06.038.
2. M. Katsnelson, V.Y. Irkhin, L. Chioncel, A. Lichtenstein, and R.A. de Groot. Rev. Mod. Phys. **80**, 315 (2008). doi:10.1103/RevModPhys.80.315.
3. A. Birsan and V. Kuncser. J. Magn. Magn. Mater. **388**, 1 (2015). doi:10.1016/j.jmmm.2015.04.007.
4. R. de Groot, F. Mueller, P. van Engen, and K. Buschow. Phys. Rev. Lett. **50**, 2024 (1983). doi:10.1103/PhysRevLett.50.2024.
5. R. Helmholdt, R. de Groot, F. Mueller, P. van Engen, and K. Buschow. J. Magn. Magn. Mater. **43**, 249 (1984). doi:10.1016/0304-8853(84)90075-1.
6. S. Ishida, S. Fujii, S. Kashiwagi, and S. Asano. J. Phys. Soc. Jpn. **64**, 2152 (1995). doi:10.1143/JPSJ.64.2152.
7. V. Alijani, S. Ouardi, G.H. Fecher, et al. Phys. Rev. B, **84**, 224416 (2011). doi:10.1103/PhysRevB.84.224416.
8. I. Galanakis and P. Mavropoulos. Phys. Rev. B, **67**, 104417 (2003). doi:10.1103/PhysRevB.67.104417.
9. K. Yao, G. Gao, Z. Liu, and L. Zhu. Solid State Commun. **133**, 301 (2005). doi:10.1016/j.ssc.2004.11.016.
10. W.-H. Xie, Y.-Q. Xu, B.-G. Liu, and D. Pettifor. Phys. Rev. Lett. **91**, 037204 (2003). doi:10.1103/PhysRevLett.91.037204.
11. R. Soulen, Jr., M.S. Osofsky, B. Nadgorny, et al. Science, **282**, 85 (1998). doi:10.1126/science.282.5386.85.
12. O.T. Uto, P.O. Adebambo, J.O. Akinlami, S. Kenmoe, and A G. Adebayo. Solids, **3**, 22 (2022). doi:10.3390/solids3010002.
13. M. Javed, M.A. Sattar, M. Benkraouda, and N. Amrane. Opt. Quant. Electron. **54**, 1 (2022). doi:10.1007/s11082-021-03373-1.
14. E. G. Özdemir and Z. Merdan. J. Magn. Magn. Mater. **491**, 165567 (2019). doi:10.1016/j.jmmm.2019.165567.
15. M. K. Hussain. *In* Spin world scientific. 2019. p. 1950018.
16. L. Feng, E. Liu, W. Zhang, W. Wang, and G. Wu. J. Magn. Magn. Mater. **351**, 92 (2014). doi:10.1016/j.jmmm.2013.09.054.
17. P. Blaha, K. Schwarz, P. Sorantin, and S. Trickey. Comput. Phys. Commun. **59**, 399 (1990). doi:10.1016/0010-4655(90)90187-6.
18. P. Blaha, K. Schwarz, G. K. Madsen, D. Kvasnicka, and J. Luitz. An augmented plane wave+ local orbitals program for calculating crystal properties. Northwestern University, Evanston, IL. 2001. p. 60.
19. J.P. Perdew, K. Burke, and Y. Wang. Phys. Rev. B, **54**, 16533 (1996). doi:10.1103/PhysRevB.54.16533.
20. J.P. Perdew, K. Burke, and M. Ernzerhof. Phys. Rev. Lett. **77**, 3865 (1996). doi:10.1103/PhysRevLett.77.3865.
21. H.C. Kandpal, G.H. Fecher, and C. Felser. J. Phys. D Appl. Phys. **40**, 1507 (2007). doi:10.1088/0022-3727/40/6/S01.
22. F. Murnaghan. America, **30**, 244 (1944). doi:10.1073/pnas.30.9.244.
23. S.J. Clark, M.D. Segall, C.J. Pickard, P.J. Hasnip, M.I. Probert, K. Refson, and M.C. Payne. Z. Kristallogr. Cryst. Mater. **220**, 567 (2005). doi:10.1524/zkri.220.5.567.65075.

24. A. Gherriche, A. Bouhemadou, Y. Al-Douri, S. Bin-Omran, R. Khenata, and M. Hadi. Mater. Sci. Semicond. Process. **131**, 105890 (2021). doi:10.1016/j.mssp.2021.105890.
25. R. Fürth. *In* Mathematical Proceedings of the Cambridge Philosophical Society. Cambridge University Press, 1941. pp. 34.
26. F. Mouhat and F.-X. Coudert. Phys. Rev. B, **90**, 224104 (2014). doi:10.1103/PhysRevB.90.224104.
27. S. Pugh. Lond. Edinb. Dublin Philos. Mag. J. Sci. **45**, 823 (1954). doi:10.1080/14786440808520496.
28. P. Ravindran, L. Fast, P.A. Korzhavyi, B. Johansson, J. Wills, and O. Eriksson. J. Appl. Phys. **84**, 4891 (1998). doi:10.1063/1.368733.
29. Y. Cao, J. Zhu, Y. Liu, Z. Nong, and Z. Lai. Comput. Mater. Sci. **69**, 40 (2013). doi:10.1016/j.commatsci.2012.11.037.
30. D. Vanderbilt. Phys. Rev. B, **41**, 7892 (1990). doi:10.1103/PhysRevB.41.7892.
31. G. Kresse and J. Hafner. Phys. Rev. B, **49**, 14251 (1994). doi:10.1103/PhysRevB.49.14251.